frontiers in Materials

ORIGINAL RESEARCH
published: 25 April 2018
doi: 10.3389/fmats.2018.00025

Hybrid Nanomaterials of Magnetic Iron Nanoparticles and Graphene Oxide as Matrices for the Immobilization of β-Glucosidase: Synthesis, Characterization, and Biocatalytic Properties

*Georgios Orfanakis[1], Michaela Patila[1], Alexandra V. Catzikonstantinou[1], Kyriaki-Marina Lyra[2], Antonios Kouloumpis[2], Konstantinos Spyrou[2], Petros Katapodis[1], Alkiviadis Paipetis[2], Petra Rudolf[3], Dimitrios Gournis[2] and Haralambos Stamatis[1]**

[1] Biotechnology Laboratory, Department of Biological Applications and Technologies, University of Ioannina, Ioannina, Greece, [2] Department of Material Science and Engineering, University of Ioannina, Ioannina, Greece, [3] Faculty of Science and Engineering, Zernike Institute for Advanced Materials, University of Groningen, Groningen, Netherlands

OPEN ACCESS

Edited by:
Emilia Morallon,
University of Alicante, Spain

Reviewed by:
Anna Maria Ferretti,
Institute of Molecular Science and Technologies (CNR), Italy
Ángel Berenguer-Murcia,
University of Alicante, Spain

***Correspondence:**
Haralambos Stamatis
hstamati@uoi.gr

Specialty section:
This article was submitted to Carbon-Based Materials, a section of the journal Frontiers in Materials

Received: 03 January 2018
Accepted: 09 April 2018
Published: 25 April 2018

Citation:
Orfanakis G, Patila M, Catzikonstantinou AV, Lyra K-M, Kouloumpis A, Spyrou K, Katapodis P, Paipetis A, Rudolf P, Gournis D and Stamatis H (2018) Hybrid Nanomaterials of Magnetic Iron Nanoparticles and Graphene Oxide as Matrices for the Immobilization of β-Glucosidase: Synthesis, Characterization, and Biocatalytic Properties. Front. Mater. 5:25. doi: 10.3389/fmats.2018.00025

Hybrid nanostructures of magnetic iron nanoparticles and graphene oxide were synthesized and used as nanosupports for the covalent immobilization of β-glucosidase. This study revealed that the immobilization efficiency depends on the structure and the surface chemistry of nanostructures employed. The hybrid nanostructure-based biocatalysts formed exhibited a two to four-fold higher thermostability as compared to the free enzyme, as well as an enhanced performance at higher temperatures (up to 70°C) and in a wider pH range. Moreover, these biocatalysts retained a significant part of their bioactivity (up to 40%) after 12 repeated reaction cycles.

Keywords: bioconjugate, immobilization, graphene, magnetic nanoparticles, nanoscaffold

INTRODUCTION

Over the last decades, nanobiotechnology, which combines the synergistic interactions between nanotechnology and biotechnology, has been an emerging field for the design of innovative nanosystems with potential applications in biosensing, bioenergy, bio-imaging, and biocatalysis (Verma et al., 2012). In biocatalysis, the development of novel nanobiocatalytic systems through the immobilization of enzymes on nanoscale materials attracted much scientific interest and their potential for applications in various industrial fields were recognized. The immobilization of enzymes on nano-sized materials leads to desirable nanobiocatalysts due to the higher enzyme loading capacity achieved, the enhanced mass transfer efficiency, and the stabilization that nanomaterials provide (Pavlidis et al., 2012b; Patila et al., 2016b).

Among the different types of nanomaterials used for this purpose, carbon-based materials such as graphene, a two-dimensional (2D) carbon sheet with single-atom thickness, and graphene oxide (GO), its oxidized derivative, have been used for enzyme immobilization (Pavlidis et al., 2014). Their distinctive characteristics in terms of surface structure, excellent electrical, chemical, and mechanical properties, as well as their ability to affect the microenvironment of biomolecules

like proteins make them ideal supports for enzyme immobilization (Zhang et al., 2010; Pavlidis et al., 2012a, 2014). Moreover, the possibility to further functionalize their surface with desirable functional groups (such as epoxide, carboxylic, hydroxyl, and amine groups) results in the specific/targeted immobilization of the enzymes (Li et al., 2013; Sehat et al., 2015; Patila et al., 2016a). Several studies have been carried out to investigate the covalent or non-covalent immobilization of various enzymes on GO-based nanomaterials (Shen et al., 2010; Hermanová et al., 2015).

On the other hand, magnetic nanoparticles represent a family of nanoscale materials of great interest that have been broadly utilized as carriers for enzyme immobilization (Xu et al., 2014; Ahmad and Sardar, 2015). Magnetic nanoparticles are a class of particulate materials (size <100 nm) that can be handled under the influence of a magnetic field. They usually consist of magnetic cores, such as iron, nickel, cobalt, or their oxides such as magnetite (Fe_3O_4), maghemite (γ-Fe_2O_3), cobalt ferrite (Fe_2CoO_4), chromium di-oxide (CrO_2) (Indira, 2010). Enzyme immobilization on magnetic nanoparticles provides substantial competitive advantages such as a high specific surface that increases the amount of bound enzyme, less mass transfer resistance and fouling, but also simple and selective separation of the immobilized enzymes from the reaction medium through the implementation of an external magnetic field (Huang et al., 2003). The functionalization of magnetic nanoparticles with carbon-based nanomaterials has recently attracted great interest as the resulting hybrid nanomaterials combine the properties of both building blocks. These hybrids can be applied in enzyme immobilization (Jiang et al., 2012; Gokhale et al., 2013) as well as in drug delivery (Yang et al., 2009; Mahmoudi et al., 2011).

In the present study, hybrid nanomaterials of magnetic iron nanoparticles and GO, as well GO-derivatives, were synthesized and used as nanosupports for the covalent immobilization of β-glucosidase. β-Glucosidases (β-D-glucoside glucohydrolase, EC 3.2.1.21) are found in both prokaryote and eukaryote organisms, where they catalyze the hydrolysis of glycosidic bonds of disaccharides, oligosaccharides, and alkyl- and aryl β-glucosides under physiological conditions. Moreover, under certain conditions, they catalyze the synthesis of glycosyl bonds (Bhatia et al., 2002; Chang et al., 2013). β-Glucosidases (bgl) are well-characterized, biologically important enzymes, and have potential for many biotechnological applications, such as biofuel and ethanol production, flavor improvement, and release of aromatic compounds in wine making (Singh et al., 2016; Ahmed et al., 2017). The aim of this work focuses on the investigation of the effect of structural characteristics deriving from different synthetic procedures of hybrid GO-magnetic nanoparticles on the catalytic behavior of bgl. The synergistic interactions between magnetic iron nanoparticles and GO and their effect on the catalytic properties (activity, stability, reusability) of the enzymes are still under investigation giving rise to a continuously evolving field. The novel hybrid GO-magnetic nanoparticle nanostructures formed were characterized by X-ray diffraction (XRD) and thermogravimetrc analysis (TG/DTA), while the nanobiocatalysts formed (the hybrid GO-magnetic nanoparticle nanostructures containing β-glucosidase) were studied by atomic force microscopy (AFM). The investigation of the catalytic behavior, the thermal stability, and the reusability of these novel nanobiocatalysts indicated that they can be effectively used for β-glucosidase immobilization, resulting in robust nanobiocatalysts with potential applications in various biocatalytic processes.

MATERIALS AND METHODS

β-Glucosidase (bgl) from almonds was purchased from Sigma–Aldrich (St. Louis, MO) and used without further purification. The Glucose Assay Kit was purchased from Sigma–Aldrich (St. Louis, MO). *p*-Nitrophenyl-β-D-glucopyranoside (*p*NPG), (3-aminopropyl)triethoxysilane (APTES), nitric acid (65%), potassium chloride, oleylamine (98%), and Iron(III)Nitrate nanohydrate (98%) were purchased from Sigma–Aldrich (St. Louis, MO). Glutaraldehyde solution 25% for electron Microscopy was purchased from Merck KGaA Darmstadt, Germany. Graphite (purum powder, ≤0.2 mm) was purchased from Fluka. Sulfuric acid (95–97%) and absolute ethanol (100%) were purchased from Merck.

Synthesis

Synthesis of GO

Graphene oxide aqueous dispersions were synthesized from graphite powder as reported elsewhere (Staudenmaier, 1898; Enotiadis et al., 2012). Briefly, 5 g of graphite powder were added to a solution consisting of 200 mL of H_2SO_4 (95–97%) and 100 mL of HNO_3 (65%) while cooling in a bath (0°C). To this solution, powdered $KClO_3$ (100 g) was added slowly under continuous stirring and cooling. After 18 h the oxidation product was washed with distilled water until the pH reached 6. The final product was dried at room temperature.

Synthesis of GO-C_2-NH_2

GO was further functionalized with ethylene diamine to provide free $-NH_2$ groups on its surface (this product was labeled GO-C_2-NH_2). Two hundred and fifty milligrams of GO were dispersed in 250 mL of distilled water and left under stirring for 24 h at room temperature. At the same time, 750 mg ethylene diamine was dissolved in 250 mL distilled water. The ethylene diamine solution was added dropwise to the GO dispersion and the mixture was incubated at room temperature for 24 h. The modified GO was washed with distilled water, separated by centrifugation, and air-dried at room temperature.

Synthesis of γ-Fe_2O_3 Nanoparticles (γFe)

Organophilic iron nanoparticles were prepared using a thermolysis method based on the thermolytic decomposition of an iron nitrate precursor [Fe(Nitrate)], using oleylamine (OA) both as a solvent and a capping agent (Tzitzios et al., 2007, 2008). In a typical synthesis of small-scale nanoparticles, 0.25 g [Fe(Nitrate)] were dispersed in 20 mL oleylamine at 80°C for 30 min, under continuous magnetic stirring. When the mixture became a clear solution, the temperature was raised at 250°C for 1 h. Then, the reaction mixture was allowed to cool to room temperature. The dark brown iron nanoparticles were washed with 50 mL ethanol and the precipitate was isolated by

centrifugation at 4,000 rpm for 5 min and left to dry at room temperature (this product was labeled as γFe-OA and used further for the hybridization with GO as described below). The synthesized nanoparticles were further dispersed in an acetic acid solution (50 wt%) in order to remove the oleylamine and obtain the pristine iron nanoparticles. The mixture was stirred for 2 h and then washed several times with distilled water and dried at room temperature (this product was labeled as γFe).

Synthesis of GO-Oleylamine- γ-Fe_2O_3 (GO-OA-γFe)

GO was firstly modified with oleylamine (OA) to create organophilic graphite oxide (Yang et al., 2012). In a typical procedure, 300 mg GO were dissolved in 150 mL distilled water and stirred for 24 h. At the same time, 0.9 g oleylamine were dispersed in 50 mL ethanol. The oleylamine solution was added dropwise to the GO dispersion. The new suspension was stirred for 24 h, followed by four washes with a 50% solution of water/ethanol. The GO derivative was air-dried at room temperature. For the synthesis of the hybrid nanoparticle, 9 mg γ-Fe functionalized with oleylamine (γFe-OA) were dissolved in 20 mL $CHCl_3$ and placed in an ultrasonic bath for 5 min. At the same time 3 mg GO-OA were added in 30 mL $CHCl_3$ and sonicated for 5 min. The GO-OA-γFe was synthesized by addition of the GO-OA solution to the γFe-OA solution and incubation for 24 h under stirring. Finally, the resulted material was washed several times with chloroform and dried at room temperature.

Synthesis of GO-γ-Fe_2O_3 (GO-γFe)

In situ synthesis of the hybrid nanomaterial GO-γFe took place through the following procedure (Xu et al., 2008); 50 mg GO were dispersed in 30 mL ethanol and 600 mg [Fe(Nitrate)] were dispersed in 20 mL ethanol. The two solutions were mixed under stirring for 30 min. Thereafter the mixture was heated at 100°C under continuous stirring for 1 h. After cooling to room temperature, the hybrid nanoparticles were centrifuged and washed with ethanol several times, to clean the nanoparticles from any impurities.

Characterization

Atomic Force Microscopy Studies

AFM images were obtained in tapping mode with a 3D Multimode Nanoscope, using Tap-300G silicon cantilevers with a tip radius < 10 nm and a force constant of $\approx$ 20–75 N m^{-1}. Samples were deposited onto silicon wafers (P/Bor, single side polished) from aqueous solutions by drop casting.

X-Ray Diffraction Analysis

XRD patterns of γFe nanoparticles and all carbon nanostructures were collected on a D8 Advance Bruker diffractometer with Cu Kα radiation (40 kV, 40 mA) and a secondary-beam. The core size of nanoparticles was calculated using the Scherrer equation and the interlayer distance was calculated using Bragg equation (Bragg and Bragg, 1913).

TG/DTA Analysis

Thermogravimetric analysis (TG) and differential thermal analysis (DTA) were performed using a PerkinElmer Pyris Diamond TG/DTA instrument. Samples of approximately 3–3.5 mg were heated under air flow gas (100 mL/min) from 30 to 800°C, with a 5°C/min heating rate.

FTIR Measurement

FTIR spectra in the range of 400–4,000 cm^{-1} were measured with a FTIR-8400 infrared spectrometer (Shimadzu, Tokyo, Japan) equipped with a deuterated triglycine sulfate (DTGS) detector. A total of 64 scans were averaged for each sample with 2 cm^{-1}, using KBr pellets containing *ca.* 2 wt% sample.

Immobilization

Covalent Immobilization of bgl on GO-C_2-NH_2

In a typical procedure, 15 mg GO-C_2-NH_2 were added in the appropriate volume of citrate-phosphate buffer (100 mM, pH 5.0) and sonicated for 30 min. Glutaraldehyde was then added at a final concentration of 0.1 M and the solution was incubated for 1.5 h at 30°C, under constant stirring. Thorough centrifugation followed to remove the glutaraldehyde excess. The activated GO-C_2-NH_2 was re-dispersed in 8 mL citrate-phosphate buffer (100 mM, pH 5.0) and sonicated for 10 min. 7.5 mg of bgl were added to the solution and the mixture was incubated for 1.5 h at 30°C, under constant stirring. The solution was centrifuged, washed with citrate-phosphate buffer (100 mM, pH 5.0) and dried over silica gel. This product was labeled bgl/GO-C_2-NH_2.

Covalent Immobilization of bgl on GO-OA-γFe

In a typical procedure, 8 mg of GO-OA-γFe were added to the appropriate volume of citrate-phosphate buffer (100 mM, pH 5.0) and sonicated for 30 min. Glutaraldehyde was then added at a final concentration of 0.5 M and the solution was incubated for 1.5 h at 30°C, under constant stirring. Thorough centrifugation followed to remove the glutaraldehyde excess. The activated nanomaterial was then re-dispersed in 6 mL citrate-phosphate buffer (100 mM, pH 5.0) and sonicated for 10 min. 2.5 mg of bgl was added to the nanomaterial solution and the mixture was treated as described for the immobilization on GO-C_2-NH_2. This product was labeled bgl/GO-OA-γFe.

Covalent Immobilization of bgl on GO-γFe and γFe

The nanomaterials were firstly modified with APTES to add terminal amine groups on their surface. In a typical procedure, 7.9 or 15 mg GO-γFe or γFe, respectively, were dispersed in 1.5 mL ethanol and sonicated for 30 min. 0.3 mL APTES was added to the solutions and incubated at 25°C for 24 h. The solutions were centrifuged and washed with distilled water various times. The functionalized nanomaterials were re-dispersed in citrate-phosphate buffer (100 mM, pH 5.0). Glutaraldehyde was added to the solutions at a final concentration of 0.5 M, and the mixtures were incubated for 24 h at 30°C. Centrifugation and several washes followed to remove the glutaraldehyde excess. The activated nanomaterials were re-dispersed in 6 mL citrate-phosphate buffer (100 mM, pH 5.0) and 8.6 or 7.2 mg of the enzyme was added to the GO-γFe or γFe solution, respectively. The mixtures were incubated at 25°C for 24 h, under constant stirring. The immobilized enzyme was separated by centrifugation and the

mixtures were treated as described for the immobilization on GO-C_2-NH_2. The products were labeled bgl/GO-γFe and bgl/γFe.

Determination of Immobilization Yield

The amount of immobilized enzyme was determined by calculating the protein concentration in the supernatant after the immobilization procedure using the Bradford method (Bradford, 1976). Loading was estimated as the difference between the amount of protein in the supernatant after immobilization and the amount of initial protein.

Determination of Free and Immobilized bgl Activity

The enzymatic reaction (0.02 mg/mL free or immobilized bgl) was performed at 40°C, in citrate-phosphate buffer (100 mM pH 5.0), with reaction time of 10 min. Two millimolars *p*NPG were added and the reaction was stopped with the addition of 0.5 mL Na_2CO_3 (10% w/v). The activity of bgl was measured using *p*NPG as a substrate which is converted to a colored product p-nitrophenol (pNP). The concentration of *p*NPG in the reaction mixture was 2 mM. The enzymatic reaction was stopped after 10 min with the addition of 0.5 mL Na_2CO_3 (10% w/v). The activity of bgl was determined by measuring the pNP concentration at 410 nm using appropriate standard curve. One bgl unit (U) was defined as the amount of enzyme required to release 1 μmol of pNP per minute under above experimental conditions.

The effect of temperature was studied by measuring the activity of both free and immobilized bgl at different temperatures (ranging from 30 to 75°C). Similarly, the effect of pH was studied by measuring the activity of both free and immobilized bgl at pH values ranging from 4.0 to 6.0.

Stability

Free or immobilized bgl (0.02 mg/mL) was incubated in citrate-phosphate buffer (100 mM, pH 5.0) at 60°C. The half-time constants were calculated by measuring the remaining activity through the *p*NPG hydrolysis as described before. In the case of immobilized enzyme, the samples were first sonicated to achieve a well-dispersed mixture.

Reusability of Immobilized bgl

The enzymatic hydrolysis of *p*NPG was chosen as test case in order to investigate the reusability of immobilized bgl. The reaction mixture (1 mL) contained 2 mM *p*NPG in citrate-phosphate buffer (100 mM, pH 5.0) and 0.02 mg/mL of immobilized bgl; it was incubated at 50°C under stirring at 800 rpm for 24 h. After each reaction cycle, the immobilized bgl was separated by centrifugation and washed three times with citrate-phosphate buffer (100 mM, pH 5.0). Immobilized bgl was repeatedly used 12 times. The activity determined in the first cycle was taken as control (100%) for the calculation of remaining activity (in percent).

RESULTS AND DISCUSSION

Characterization of the Synthesized Nanomaterials by XRD

A first indication about the structure and size of the synthesized iron nanoparticles (γ-Fe) can be gained from the X-ray diffraction data shown in **Figure 1**. The peaks appearing in the range of 20° and 80° can be assigned to the crystallographic Miller planes [211], [220], [311], [400], [422], [511], [440]; more specifically, the iron nanoparticles show the spinel structure with JCPDS No: 04-0755. **Table 1** illustrates the position of peaks (degrees) and the size of iron nanoparticles as calculated by applying the Scherrer equation. From **Table 1**, the average core size of the nanoparticles was calculated to amount to 4.95 ± 0.51 nm.

Figure 2 displays a comparison of the X-ray diffraction patterns from the synthesized carbon materials GO, GO-OA, and GO-C_2-NH_2 as well as from the hybrid nanostructures GO-γFe and GO-OA-γFe. Supplementary information presents the whole XRD graphs of GO-γFe and GO-OA-γFe where the Miller planes [311], [533] for GO-γFe, and [311] for GO-OA-γFe, of maghemite (γ-Fe_2O_3) can be observed (Figure S1 in Supplementary Material). For GO the peak located at 11.23° corresponds to the 001 reflection of adjacent graphene layers; after the interaction of oleylamine and ethylene diamine molecules with graphene oxide (GO-OA, GO-C_2-NH_2) this peak

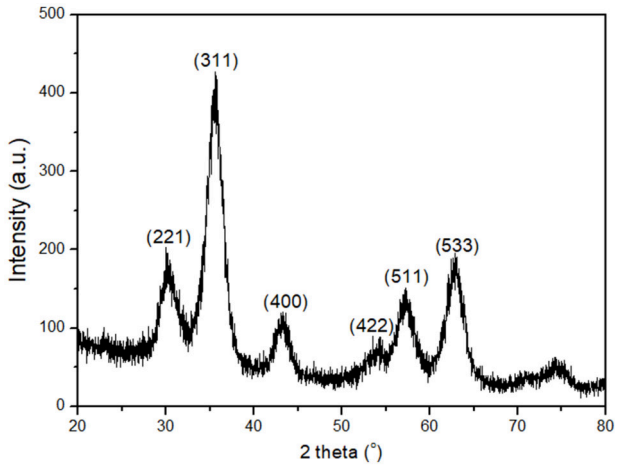

FIGURE 1 | X-Ray diffraction pattern of the γFe nanoparticles.

TABLE 1 | The position of peaks (degrees) and the size of γFe nanoparticles.

Degrees (°)	Core size of iron nanoparticles, d (nm)
30.14	4.88 ± 0.36
35.69	4.33 ± 0.29
43.19	5.55 ± 0.13
57.11	4.97 ± 0.24
62.90	5.03 ± 0.62

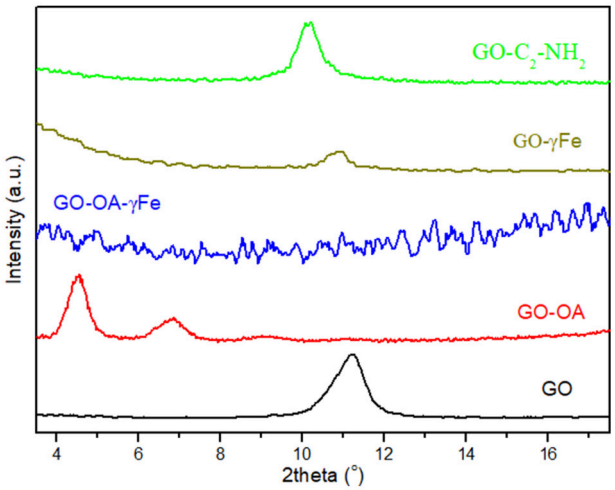

FIGURE 2 | X-Ray diffraction for the nanomaterials GO, GO-OA, GO-OA-γFe, GO-γFe, and GO-C_2-NH_2.

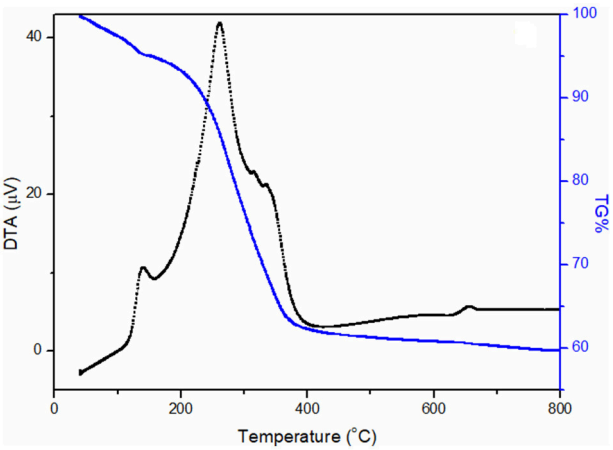

FIGURE 3 | Thermal (DTA, black) and thermogravimetric (TG%, blue) analysis of γFe nanoparticles.

is seen to have shifted to lower angles. More specifically 4.5° for GO-OA and 10.8 for GO-C_2-NH_2, indicating the successful intercalation of oleylamine and ethylene diamine between the interlamellar galleries of GO. Due to this intercalation the interlayer distance between graphene layers increased from a basal spacing of $d_{001} = 7.9$ Å for GO (determined by the oxygen containing functional groups) to a basal spacing of $d_{001} = 19.6$ Å for GO-OA and $d_{001} = 8.6$ Å for GO-C_2-NH_2. Furthermore, in **Figure 2** (blue line), one notes that the (001) reflection is not observed in the case of the GO-OA-γFe hybrid material, possibly due to the total exfoliation of the graphene layers after the interaction with the γFe nanoparticles. Moreover, the hybrid material GO-γFe (olive green) seems to maintain its layered structure, meaning that γFe nanoparticles attached only on the surface of the layered GO.

TG/DTA Analysis of the Synthesized Nanomaterials

In order to estimate the functionalization yield of the γFe nanoparticles we carried out differential thermal analysis (DTA) and determined the mass loss. **Figure 3** shows the DTA curve and the corresponding mass loss (TG %) and exhibits an exothermic DTA peaks at around 130 and 262°C, which are assigned to the adsorbed water on the γ-iron oleylamine nanoparticles and the removal of oleylamine, respectively (see Supplementary Material). This same removal of oleylamine gives also rise to the weight loss observed from 198 to 386°C in the TG% curve that allows to estimate the organic part as 39 wt%.

AFM Measurements

To confirm the size of the γFe nanoparticles and collect direct evidence for the immobilization of bgl on γFe nanoparticles, we collected AFM height images of these samples depositited on a Si-wafer; the micrographs are shown in **Figure 4**. Relatively isolated and uniform γFe particles and bgl/γFe conjugates without aggregation can be observed. The average heights of the pristine γFe and the immobilized enzyme range in the areas of 2.5–4.5 nm estimated by an average count size of at least 100 particles, (see Supplementary material, Figure S3) and 13–14 nm, respectively, as derived from the topographical height profile (section analysis) indicating the successful attachment of bgl to the nanoparticles.

Moreover, AFM height images of GO-γFe and bgl immobilized on GO-γFe, both deposited on a Si-wafer, are shown in **Figure 5**. In the left top panel few micrometers large GO flakes covered with spherical objects are clearly visible; the average height of these spheres as derived from topographical height profile was 3 nm, which agrees with the diameter of the γFe nanoparticles as determined from the XRD patterns and hence proves the successful decoration of the GO with the γFe nanoparticles. In the center and right top panels bgl molecules are observed on the surface of the hybrid GO-γFe; the size of the attached bgl on the GO sheets is estimated between 16 and 25 nm. This size is much larger than the size of a single bgl molecule, indicating that agglomeration must have occurred upon protein immobilization. In both cases, the average thickness of the GO flakes is found to be 0.8 nm, which corresponds to the thickness of a single graphene oxide layer.

A typical AFM image of bgl/GO-C_2-NH_2 deposited on a Si-wafer is shown in **Figure 6**. Isolated nanosheets with an average thickness of 0.85 nm are observed (as calculated from the cross section analysis), which identifies them as single graphene oxide layers functionalized with C-NH_2. Moreover the surface of the nanosheets shows a uniform and dense coverage with bgl molecules, revealing the successful protein immobilization.

Immobilization Yield and Activity of Immobilized bgl

In the present study, functionalized GO, magnetic nanoparticles (γFe) as well as hybrid nanomaterials of γFe and GO were used as nanosupports for the covalent immobilization of β-glucosidase. In the cases of γFe and GO-γFe, further functionalization with APTES was performed in order to add free amine

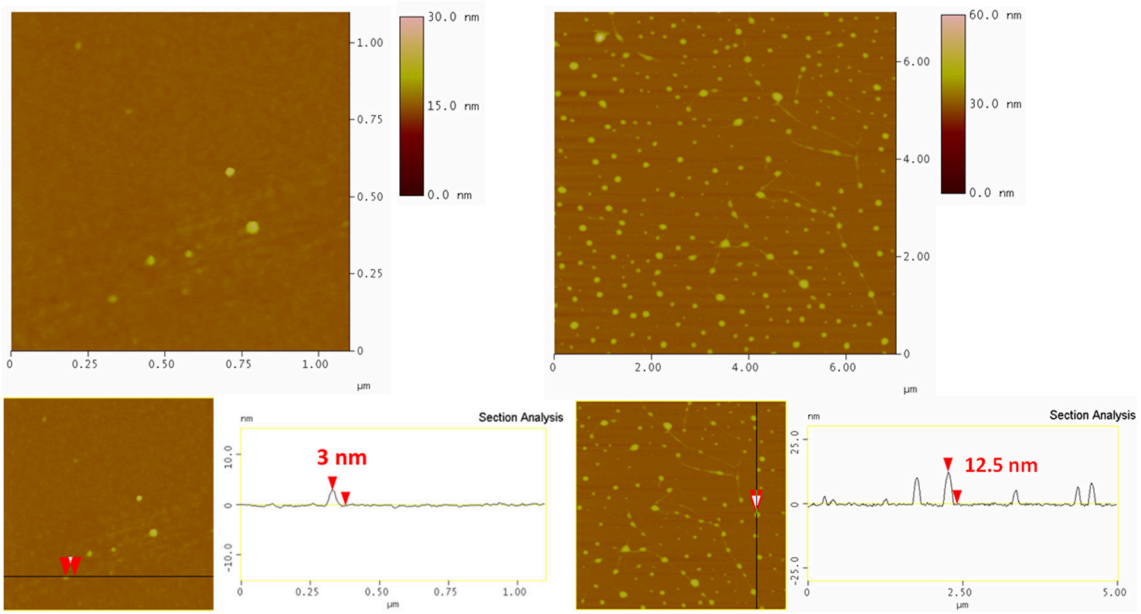

FIGURE 4 | AFM height images **(Top)** and cross section analysis **(Bottom)** of γFe nanoparticles **(Left)** and bgl/γFe **(Right)**.

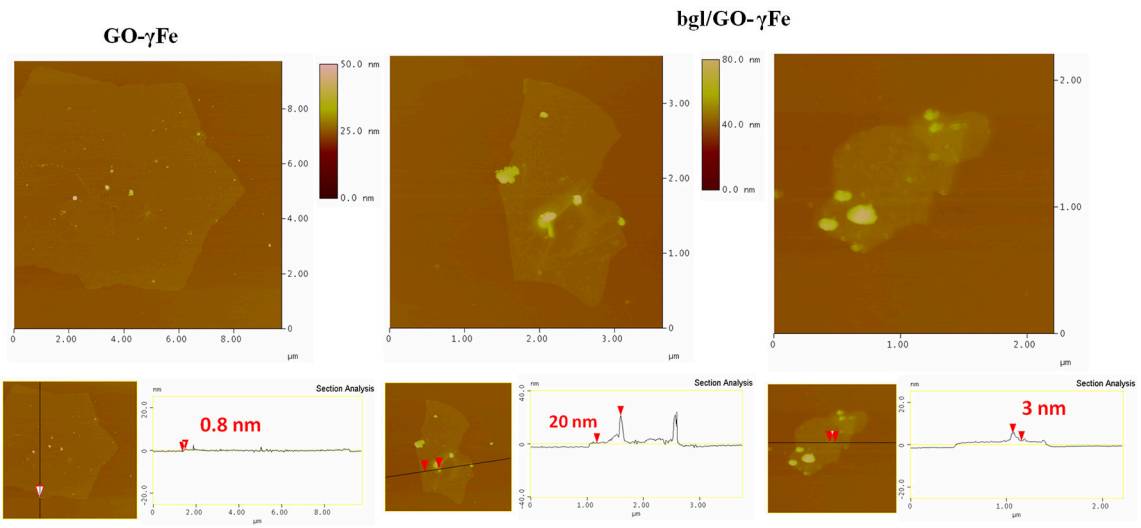

FIGURE 5 | AFM height images **(Top)** and cross section analysis **(Bottom)** of GO-γFe nanoparticles **(Left)** and bgl/GO-γFe **(Center and Right)**.

groups on the surface of the nanomaterials for the cross-linking with the free amine groups on the surface of the enzyme. The successful functionalization of the nanomaterials with APTES was confirmed by FTIR spectroscopy (Figure S4 in Supplementary Material). The highest immobilization yields for grafting bgl to different supports, as well as the activities of free and immobilized bgl are presented in **Table 2**. It is expected that the structural characteristics of a nanomaterial, namely composition, size, surface area, functional groups and geometry, affect the immobilization yield, and the enzyme activity (Pavlidis et al., 2014). Moreover, the enzyme to support mass ratio could also affect the immobilization efficiency and the activity of immobilized enzymes (Pavlidis et al., 2012b; Samaratunga et al., 2015). In the present work, various enzyme to support mass ratios, ranging from 0.3 to 1.1, have been tested in order to optimize the immobilization yield and activity of bgl (data not shown). The optimal ratios, regarding the activity of immobilized enzyme, are described in the Materials and Methods section.

The immobilization yield of β-glucosidase apparently depends on the nature of the nanomaterial used. More

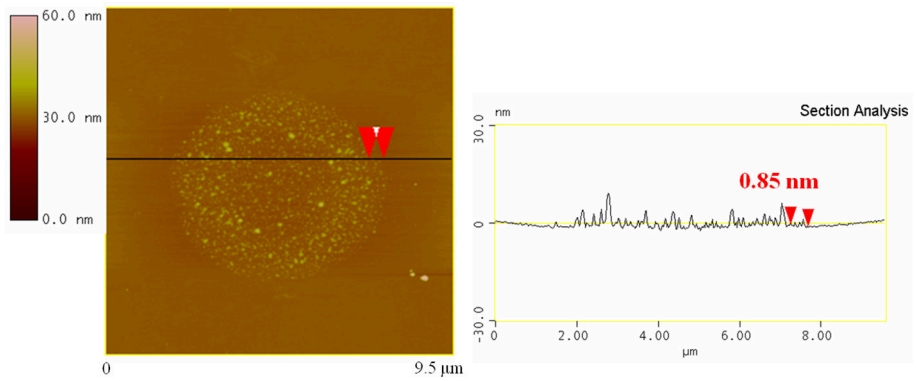

FIGURE 6 | AFM micrograph **(Left)** and cross section analysis **(Right)** of bgl/GO-C_2-NH_2.

TABLE 2 | Activity of free and immobilized bgl and immobilization yield (%) of bgl, calculated as the concentration ratio of protein immobilized on nanomaterials to the initial protein quantity used (standard deviation was less than 3% in all cases).

Sample	U/mg protein	Immobilization yield (%)
Free enzyme	5.66	–
bgl/GO-C_2-NH_2	0.02	32.4
bgl/GO-OA-γFe	2.14	37.7
bgl/γFe	1.76	65.0
bgl/GO-γFe	2.83	69.5

specifically, the highest immobilization efficiency was observed for bgl on iron-based nanomaterials, rather than on functionalized GO. Similar immobilization efficiencies have been previously reported for bgl on magnetic nanoparticles (Ricco et al., 2014) or GO-iron nanoparticles hybrid nanomaterials (Gokhale et al., 2013; Ricco et al., 2014). It is interesting to note that the type of amine groups on the surface of the hybrid nanomaterial seems to affect the immobilization efficiency. In the case of bgl/GO-OA-γFe, the enzyme covalently binds to the secondary amines of oleylamine, while for bgl/GO-γFe, bgl binds to the free terminal amine groups of APTES. The higher immobilization yield observed for bgl/GO-γFe might derive from the higher accessibility of the free primary amines of APTES.

The catalytic activity of immobilized bgl is lower than that of free enzyme (**Table 2**). The covalent immobilization is known to affect the activity of the enzymes, due to conformational changes produced by the grafting (Patila et al., 2016a). It must be noted that the catalytic activity of the immobilized bgl does not seem to depend on the enzyme loading. This observation could be attributed to the different interactions between enzyme and nanomaterials that could affect the availability of the active sites of the enzyme to the substrate molecules, and thus the expressed activity of the immobilized biocatalyst (Pavlidis et al., 2014).The lowest activity was observed in the case of bgl/GO-C_2-NH_2, which correlates with the low enzyme loading on this nanomaterial. On the contrary, the highest activity of immobilized bgl was achieved when graphene oxide and iron nanoparticles were used together as hybrid immobilization matrices. The high surface area of GO leads to specific interactions with the enzyme, which may induce conformational changes in the protein, leading to an increased hydrolytic activity (Serefoglou et al., 2008; Patila et al., 2013). Moreover, the small size of iron nanoparticles, as well as their high specific surface area, increases the flexibility of the enzyme, which in turn induces a high hydrolytic activity (Abraham et al., 2014). This specific combination of interactions with the protein molecules probably does not occur for bgl/γFe alone or for bgl/GO-C_2-NH_2, where the activity of bgl is consequently lower.

Effect of Temperature and pH on the Activity of Immobilized bgl

The enzyme activity of free and immobilized bgl was determined at various temperatures ranging from 30 to 80°C; the results are shown in **Figure 7A**. In all cases studied, the immobilized bgl exhibits higher relative activity in the temperature range 30–50°C, indicating that the immobilized enzyme exhibits a better heat resistance than the free enzyme, in accordance with a previous report (Zang et al., 2014). The activity of the free bgl increased up to a temperature of 60°C, while for the immobilized enzyme an activity increase up to 70°C was registered, depending on the immobilization support used. The highest relative activity at high temperature was observed for bgl/GO-C_2-NH_2 and bgl/GO-OA-γFe, where the enzyme retained up to 100 and 50% of its activity at 70 and 80°C, respectively. This result demonstrates the effectiveness of the supports to protect the enzyme molecules at higher temperature. The shift of the optimum temperature to higher values may be attributed to conformational changes of the enzyme upon immobilization (El-Ghaffar and Hashem, 2010). A similar increase of the optimum temperature for the catalytic activity of immobilized bgl on various supports has been also reported previously (Zhou et al., 2013; Song et al., 2016).

The relation between the pH of the buffer and the catalytic activity of free and immobilized bgl is presented in **Figure 7B**. A higher enzyme activity of both the free and the immobilized

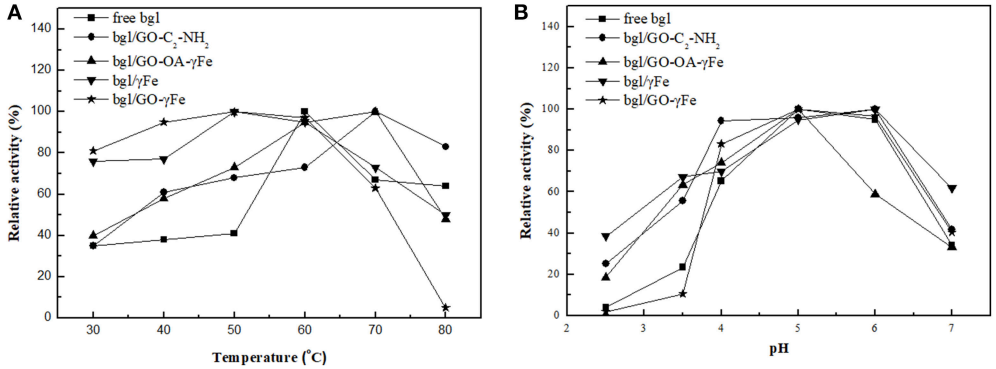

FIGURE 7 | Effect of **(A)** temperature and **(B)** pH on the relative activity of free and immobilized bgl. One hundred percentage indicates the highest activity exhibited each time either by free enzyme or the nanobiocatalyst tested.

enzyme was observed at pH 5.0; a similar pH profile has been reported for the immobilization of bgl on iron magnetic nanoparticles (Abraham et al., 2014), while other studies demonstrated that immobilized bgl on magnetic nanoparticles reaches its maximum activity at pH 4.0 (Ahmed et al., 2013; Zhou et al., 2013). In most cases, the immobilized bgl was found to keep its activity in a pH range from 2.5 to 5.0, indicating that the immobilized enzyme is less sensitive to the modification of the pH than the free enzyme. Highest pH tolerance, either in acidic or more alkaline pH values, was observed when γFe was used as immobilization support. The increased pH stability of the enzyme might be due to its covalent bonding to the support (Yuan et al., 2016).

Thermal Stability of bgl

To determine the thermal stability of free and immobilized bgl, the half-life constants, referred to the time required for the enzyme to reach 50% of its initial activity, were determined after incubation in citrate-phosphate buffer (100 mM, pH 5.0) at 60°C (**Table 3**). As it can be seen, immobilized bgl exhibited two- to four-fold higher half-times than the free enzyme. This proves that the covalent immobilization of bgl onto magnetic nanoparticles, functionalized GO, and GO-magnetic nanoparticle hybrids results in more stable biocatalysts as compared to the native soluble enzyme. A similar improvement of the stability of bgl has been reported previously, where different materials were used for the covalent immobilization of the enzyme (Ahmed et al., 2013). The observed improvement in the thermal stability of immobilized bgl comparing to the free enzyme may result from the combined action of a reduced molecular mobility and an improved conformational stabilization of the enzyme induced by the covalent bonding of bgl to the nanomaterials (Figueira et al., 2011; Patila et al., 2016a). It is interesting to note that bgl/GO-OA-γFe exhibits significant higher half-life constant than bgl/GO-γFe. The addition of the long alkyl chain of OA is expected to enhance the hydrophobic interactions between the nanosupports and the enzyme molecule, leading to a less flexible and thus more stable enzyme (Pavlidis et al., 2012b).

TABLE 3 | Half-time constants of free and immobilized bgl after incubation at 60°C.

Sample	half life (h)
Free bgl	0.66 ± 0.05
bgl/GO-C_2-NH_2	1.34 ± 0.20
bgl/GO-OA-γFe	1.70 ± 0.08
bgl/γFe	2.93 ± 0.10
bgl/GO-γFe	1.05 ± 0.15

Reuse of Immobilized bgl

The reusability of the enzymes is an important characteristic for their potential large-scale or industrial applications. Soluble enzymes cannot be separated from the reaction media and used further for more catalytic cycles. Immobilization of enzymes onto nanosupports offers the possibility to use them in repeated batches, lowering in this way the cost of the process.

To prove that this is indeed possible for immobilized bgl, our hybrid biocatalysts were applied for repeated cycles of *p*NPG hydrolysis at 50°C. As seen in **Figure 8**, the immobilized bgl retains up to 31% of its relative activity after 12 repeated reaction cycles. The reduction of the enzyme activity during repeated use might be caused by several factors, including the end-product inhibition and protein denaturation (Jordan et al., 2011; Zang et al., 2014). The remaining relative activity of the immobilized bgl depends on the nanomaterials used as supports.

The presence of iron nanoparticles onto hybrid nanomaterials of GO seems to enhance the operational stability of immobilized bgl. The highest operational stability was observed in the case of bgl/GO-OA-γFe, where the enzyme kept up to 40% of its initial activity even after 12 reaction cycles. This observation is in accordance to the beneficial effect of GO-OA-γFe on the thermal stability of bgl, as described before (**Table 3**). The combined characteristics of GO and iron nanoparticles result in the development of a larger surface area of nanosupport (Zubir et al., 2014), as the presence of γFe can act as a spacer to prevent the stacking of GO sheets, avoiding the loss of its high active surface area (Novoselov et al., 2005). Moreover, GO prevents

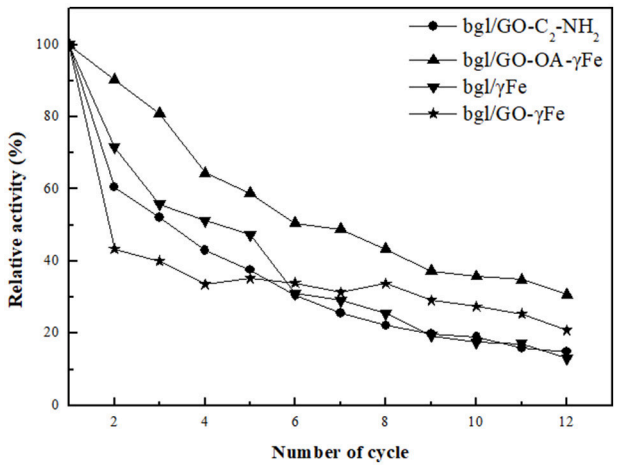

FIGURE 8 | Reusability of immobilized bgl for the hydrolysis of *p*NPG.

the agglomeration of nanoparticles and enables their distribution (He et al., 2013), leading to the formation of a large total surface area (Su et al., 2011; Song et al., 2012). The enhanced surface area of these hybrid nanomaterials could facilitate the development of specific interactions with enzyme molecules, resulting thus to the formation of more robust nanobiocatalysts.

CONCLUSIONS

Hybrid nanostructures of graphene oxide and magnetic iron nanoparticles were synthesized and used for the development of novel nanobiocatalysts through the covalent immobilization of bgl. The immobilization yield, as well as the catalytic activity of the immobilized enzyme, strongly depend on the nature of the nanomaterials used as immobilization supports. The immobilized enzyme exhibits higher thermal and operational stability, as well as higher pH and temperature tolerance, than the free enzyme. Among the nanomaterials used, GO-OA-γFe exhibits the most beneficial effect on the thermal and operational stability of the enzyme which is attributed to the presence of OA that enhances the hydrophobic interactions between the nanosupport and the enzyme molecule and thus leads to a more stable enzyme. Moreover, hybrid nanomaterials that combine GO and γFe nanoparticles result in nanosupports with enhanced total surface area that promote stronger interactions with bgl leading to the preservation of the catalytic properties of the immobilized enzyme. The high catalytic activity against various reaction conditions together with the enhanced thermal and operational stability, make these hybrids promising nanobiocatalytic systems for use in the degradation of cellulose and other biotransformations of industrial interest.

AUTHOR CONTRIBUTIONS

HS contributed to overall design of the experiments, results interpretation, and manuscript writing. DG, PR, PK, and AP designed the experimental setup and reviewed the manuscript. GO performed experiments with enzyme and results interpretation. MP and AC contributed to results interpretation, and manuscript writing. K-ML, AK, and KS performed the synthesis and characterization of materials.

ACKNOWLEDGMENTS

We acknowledge support of this work by the project Synthetic Biology: from omics technologies to genomic engineering (OMIC-ENGINE) (MIS 5002636), which is implemented under the Action *Reinforcement of the Research and Innovation Infrastructure*, funded by the Operational Programme *Competitiveness, Entrepreneurship, and Innovation* (NSRF 2014-2020) and co-financed by Greece and the European Union (European Regional Development Fund).

MP gratefully acknowledges the IKY Foundation for the financial support. The *post-doc* research was implemented with an IKY fellowship, financed by the Action of *Enhancement of post-doc researchers* from the funds of the Operational Program *Human Resources Development, Education, and Life-Long Learning* with priority axis 6,8,9 and co-funded by the European Social Fund and the Greek National Fund (MIS 5001552).

AC thanks the IKY Foundation for the financial support. The PhD research was implemented with an IKY scholarship funded by the Operational Program *Human Resources Development, Education, and Lifelong Learning*, 2014-2020, with MIS 5000432, and co-financed by the European Social Fund (ESF) and the Greek National Funds.

SUPPLEMENTARY MATERIAL

The Supplementary Material for this article can be found online at: https://www.frontiersin.org/articles/10.3389/fmats.2018.00025/full#supplementary-material

REFERENCES

Abraham, R. E., Verma, M. L., Barrow, C. J., and Puri, M. (2014). Suitability of magnetic nanoparticle immobilised cellulases in enhancing enzymatic saccharification of pretreated hemp biomass. *Biotechnol. Biofuels* 7:90. doi: 10.1186/1754-6834-7-90

Ahmad, R., and Sardar, M. (2015). Enzyme immobilization: an overview on nanoparticles as immobilization matrix. *Biochem. Anal. Biochem.* 4:178. doi: 10.4172/2161-1009.1000178

Ahmed, A., Nasim, F., Batool, K., and Bibi, A. (2017). Microbial β -glucosidase : sources, production and applications. *J. Appl. Environ. Microbiol.* 5, 31–46. doi: 10.12691/jaem-5-2-2

Ahmed, S. A., El-Shayeb, N. M. A., Hashem, A. M., Saleh, S. A., and Abdel-Fattah, A. F. (2013). Biochemical studies on immobilized fungal β-glucosidase. *Braz. J. Chem. Eng.* 30, 747–758. doi: 10.1590/S0104-66322013000400007

Bhatia, Y., Mishra, S., and Bisaria, V. S. (2002). Microbial β-glucosidases: cloning, properties, and applications. *Crit. Rev. Biotechnol.* 22, 375–407. doi: 10.1080/07388550290789568

Bradford, M. M. (1976). A rapid and sensitive method for the quantitation of microgram quantities of protein utilizing the principle dye binding. *Anal. Biochem.* 72, 248–254. doi: 10.1016/0003-2697(76)90527-3

Bragg, W. H., and Bragg, W. L. (1913). The reflection of X-rays by crystals. *Proc. R. Soc. A Math. Phys. Eng. Sci.* 88, 428–438. doi: 10.1098/rspa.1913.0040

Chang, J., Lee, Y., Fang, S., Park, D., and Choi, Y. (2013). Hydrolysis of isoflavone glycoside by immobilization of b -glucosidase on a chitosan-carbon in two-phase system. *Int. J. Biol. Macromol.* 61, 465–470. doi: 10.1016/j.ijbiomac.2013.08.014

El-Ghaffar, M. A. A., and Hashem, M. S. (2010). Chitosan and its amino acids condensation adducts as reactive natural polymer supports for cellulase immobilization. *Carbohydr. Polym.* 81, 507–516. doi: 10.1016/j.carbpol.2010.02.025

Enotiadis, A., Angjeli, K., Baldino, N., Nicotera, I., and Gournis, D. (2012). Graphene-based nafion nanocomposite membranes: enhanced proton transport and water retention by novel organo-functionalized graphene oxide nanosheets. *Small* 8, 3338–3349. doi: 10.1002/smll.201200609

Figueira, Jde. A., Dias, F. F. G., Sato, H. H., and Fernandes, P. (2011). Screening of supports for the immobilization of β -Glucosidase. *Enzyme Res.* 2011:642460. doi: 10.4061/2011/642460

Gokhale, A., Lu, J., and Lee, I. (2013). Immobilization of cellulase on magnetoresponsive graphene nano-supports. *J. Mol. Catal. B Enzym.* 90, 76–86. doi: 10.1016/j.molcatb.2013.01.025

He, G., Liu, W., Sun, X., Chen, Q., Wang, X., and Chen, H. (2013). Fe3O4@graphene oxide composite: a magnetically separable and efficient catalyst for the reduction of nitroarenes. *Mater. Res. Bull.* 48, 1885–1890. doi: 10.1016/j.materresbull.2013.01.038

Hermanová, S., Zarevucka, M., Bousa, D., Pumera, M., and Sofer, Z. (2015). Graphene oxide immobilized enzymes show high thermal and solvent stability. *Nanoscale* 7, 5852–5858. doi: 10.1039/C5NR00438A

Huang, S. H., Liao, M. H., and Chen, D. H. (2003). Direct binding and characterization of lipase onto magnetic nanoparticles. *Biotechnol. Prog.* 19, 1095–1100. doi: 10.1021/bp025587v

Indira, T. (2010). Magnetic nanoparticles: a review. *Int. J. Pharm.* 3, 1035–1042.

Jiang, B., Yang, K., Zhao, Q., Wu, Q., Liang, Z., Zhang, L., et al. (2012). Hydrophilic immobilized trypsin reactor with magnetic graphene oxide as support for high efficient proteome digestion. *J. Chromatogr. A* 1254, 8–13. doi: 10.1016/j.chroma.2012.07.030

Jordan, J., Kumar, C. S. S. R., and Theegala, C. (2011). Preparation and characterization of cellulase-bound magnetite nanoparticles. *J. Mol. Catal. B Enzym.* 68, 139–146. doi: 10.1016/j.molcatb.2010.09.010

Li, Q., Fan, F., Wang, Y., Feng, W., and Ji, P. (2013). Enzyme immobilization on carboxyl-functionalized graphene oxide for catalysis in organic solvent. *Ind. Eng. Chem. Res.* 52, 6343–6348. doi: 10.1021/ie400558u

Mahmoudi, M., Sant, S., Wang, B., Laurent, S., and Sen, T. (2011). Superparamagnetic iron oxide nanoparticles (SPIONs): development, surface modification and applications in chemotherapy. *Adv. Drug Deliv. Rev.* 63, 24–46. doi: 10.1016/j.addr.2010.05.006

Novoselov, K. S., Geim, A. K., Morozov, S. V., Jiang, D., Katsnelson, M. I., Grigorieva, I. V., et al. (2005). Two-dimensional gas of massless Dirac fermions in graphene. *Nature* 438, 197–200. doi: 10.1038/nature04233

Patila, M., Kouloumpis, A., Gournis, D., Rudolf, P., and Stamatis, H. (2016a). Laccase-functionalized graphene oxide assemblies as efficient nanobiocatalysts for oxidation reactions. *Sensors* 16, 1–14. doi: 10.3390/s16030287

Patila, M., Pavlidis, I. V., Diamanti, E. K., Katapodis, P., Gournis, D., and Stamatis, H. (2013). Enhancement of cytochrome c catalytic behaviour by affecting the heme environment using functionalized carbon-based nanomaterials. *Process Biochem.* 48, 1010–1017. doi: 10.1016/j.procbio.2013.04.021

Patila, M., Pavlidis, I. V., Kouloumpis, A., Dimos, K., Spyrou, K., Katapodis, P., et al. (2016b). Graphene oxide derivatives with variable alkyl chain length and terminal functional groups as supports for stabilization of cytochrome c. *Int. J. Biol. Macromol.* 84, 227–235. doi: 10.1016/j.ijbiomac.2015.12.023

Pavlidis, I. V., Patila, M., Bornscheuer, U. T., Gournis, D., and Stamatis, H. (2014). Graphene-based nanobiocatalytic systems: recent advances and future prospects. *Trends Biotechnol.* 32, 312–320. doi: 10.1016/j.tibtech.2014.04.004

Pavlidis, I. V., Vorhaben, T., Gournis, D., Papadopoulos, G. K., Bornscheuer, U. T., and Stamatis, H. (2012a). Regulation of catalytic behaviour of hydrolases through interactions with functionalized carbon-based nanomaterials. *J. Nanoparticle Res.* 14, 1–10. doi: 10.1007/s11051-012-0842-4

Pavlidis, I. V., Vorhaben, T., Tsoufis, T., Rudolf, P., Bornscheuer, U. T., Gournis, D., et al. (2012b). Development of effective nanobiocatalytic systems through the immobilization of hydrolases on functionalized carbon-based nanomaterials. *Bioresour. Technol.* 115, 164–171. doi: 10.1016/j.biortech.2011.11.007

Ricco, R., Doherty, C. M., and Falcaro, P. (2014). Evaluation of coupling protocols to bind beta-glucosidase on magnetic nanoparticles. *J. Nanosci. Nanotechnol.* 14, 6565–6573. doi: 10.1166/jnn.2014.9353

Samaratunga, A., Kudina, O., Nahar, N., Zakharchenko, A., Minko, S., Voronov, A., et al. (2015). Impact of enzyme loading on the efficacy and recovery of cellulolytic enzymes immobilized on enzymogel nanoparticles. *Appl. Biochem. Biotechnol.* 175, 2872–2882. doi: 10.1007/s12010-014-1463-4

Sehat, A. A., Khodadadi, A. A., Shemirani, F., and Mortazavi, Y. (2015). Fast immobilization of glucose oxidase on graphene oxide for highly sensitive glucose biosensor fabrication. *Int. J. Electrochem. Sci.* 10, 272–286.

Serefoglou, E., Litina, K., Gournis, D., Kalogeris, E., Tzialla, A. A., Pavlidis, I. V., et al. (2008). Smectit clays as solid support for immobilization of b-Glucosidase: synthesis, characterization, and biochemical properties. *Chem. Mater.* 20, 4106–4115. doi: 10.1021/cm800486u

Shen, J., Shi, M., Yan, B., Ma, H., Li, N., Hu, Y., et al. (2010). Covalent attaching protein to graphene oxide via diimide-activated amidation. *Colloids Surf. B Biointerfaces* 81, 434–438. doi: 10.1016/j.colsurfb.2010.07.035

Singh, G., Verma, A. K., and Kumar, V. (2016). Catalytic properties, functional attributes and industrial applications of b -glucosidases. *3 Biotech* 6:3. doi: 10.1007/s13205-015-0328-z

Song, Q., Mao, Y., Wilkins, M., Segato, F., and Prade, R. (2016). Cellulase immobilization on superparamagnetic nanoparticles for reuse in cellulosic biomass conversion. *AIMS Bioeng.* 3, 264–276. doi: 10.3934/bioeng.2016.3.264

Song, Y., He, Z., Hou, H., Wang, X., and Wang, L. (2012). Architecture of Fe3O4–graphene oxide nanocomposite and its application as a platform for amino acid biosensing. *Electrochim. Acta* 71, 58–65. doi: 10.1016/j.electacta.2012.03.077

Staudenmaier, L. (1898). Verfahren zur Darstellung der Graphitsäure. *Ber. Dtsch. Chem. Ges.* 31, 1481–1487. doi: 10.1002/cber.18980310237

Su, J., Cao, M., Ren, L., and Hu, C. (2011). Fe3O4 -graphene nanocomposites with improved lithium-storage and Magnetism Properties. *Education* 115, 14469–14477. doi: 10.1021/jp201666s

Tzitzios, V., Georgakilas, V., Zafiropoulou, I., Boukos, N., Basina, G., Niarchos, D., et al. (2008). A general chemical route for the synthesis of capped nanocrystalline materials. *J. Nanosci. Nanotechnol.* 8, 3117–3122. doi: 10.1166/jnn.2008.078

Tzitzios, V. K., Bakandritsos, A., Georgakilas, V., Basina, G., Boukos, N., Bourlinos, A. B., et al. (2007). Large-scale synthesis, size control, and anisotropic growth of gamma-Fe2O3 nanoparticles: organosols and hydrosols. *J. Nanosci. Nanotechnol.* 7, 2753–2757. doi: 10.1166/jnn.2007.605

Verma, M. L., Barrow, C. J., and Puri, M. (2012). Nanobiotechnology as a novel paradigm for enzyme immobilisation and stabilisation with potential applications in biodiesel production. *Appl. Microbiol. Biotechnol.* 97, 23–39. doi: 10.1007/s00253-012-4535-9

Xu, C., Wang, X., Zhu, J., Yang, X., and Lu, L. (2008). Deposition of Co3O4 nanoparticles onto exfoliated graphite oxide sheets. *J. Mater. Chem.* 18, 5625. doi: 10.1039/b809712g

Xu, J., Sun, J., Wang, Y., Sheng, J., Wang, F., and Sun, M. (2014). Application of iron magnetic nanoparticles in protein immobilization. *Molecules* 19, 11465–11486. doi: 10.3390/molecules190811465

Yang, K., Liang, S., Zou, L., Huang, L., Park, C., Zhu, L., et al. (2012). Intercalating oleylamines in graphite oxide. *Langmuir* 28, 2904–2908. doi: 10.1021/la203769p

Yang, X., Zhang, X., Ma, Y., Huang, Y., Wang, Y., and Chen, Y. (2009). Superparamagnetic graphene oxide–Fe3O4 nanoparticles hybrid for controlled targeted drug carriers. *J. Mater. Chem.* 19, 2710. doi: 10.1039/b821416f

Yuan, Y., Luan, X., Rana, X. K., Hassan, M. E., and Dou, D. (2016). Covalent immobilization of cellulase in application of biotransformation of ginsenoside Rb1. *J. Mol. Catal. B Enzym.* 133, S525–S532. doi: 10.1016/j.molcatb.2017.05.004

Zang, L., Qiu, J., Wu, X., Zhang, W., Sakai, E., and Wei, Y. (2014). Preparation of magnetic chitosan nanoparticles as support for cellulase immobilization. *Ind. Eng. Chem. Res.* 53, 3448–3454. doi: 10.1021/ie404072s

Zhang, J., Zhang, F., Yang, H., Huang, X., Liu, H., and Zhang, J. (2010). Graphene oxide as a matrix for enzyme immobilization. *Langmuir* 26, 6083–6085. doi: 10.1021/la904014z

Zhou, Y., Pan, S., Wei, X., Wang, L., and Liu, Y. (2013). Immobilization of β-glucosidase onto magnetic nanoparticles and evaluation of the enzymatic properties. *BioResources* 8, 2605–2619. doi: 10.15376/biores.8.2.2605-2619

Zubir, N. A., Yacou, C., Motuzas, J., Zhang, X., and Diniz Da Costa, J. C. (2014). Structural and functional investigation of graphene oxide-Fe3O4 nanocomposites for the heterogeneous Fenton-like reaction. *Sci. Rep.* 4:4594. doi: 10.1038/srep04594

Conflict of Interest Statement: The authors declare that the research was conducted in the absence of any commercial or financial relationships that could be construed as a potential conflict of interest.

The reviewer ÁB-M and handling Editor declared their shared affiliation.